PALEOCEANOGRAPHY, VOL. 11, NO. 6, PAGES 717-728, DECEMBER 1996

The Monterey event in the Mediterranean: A record from shelf sediments of Malta

Elizabeth Jacobs, Helmut Weissert, and Graham Shields
Geological Institute, Swiss Federal Institute of Technology, Zürich, Switzerland

Peter Stille
C.N.R.S., Centre de Géochemie de la Surface, Strasbourg, France

Abstract. Oligo-Miocene carbonate platform and shelf sediments outcropping on the Maltese Islands provide an excellent archive of the paleoceanography of the central Mediterranean. A sequence of shallow water limestones, than shelf limestones, and marls, followed again by shallow water limestones, reflects drowning of a carbonate platform, the establishment of a shelf environment and, in the late Miocene, renewed progradation and aggradation of shallow water carbonates. The sequence recording the deepening of the Maltese platform contains several phosphorite hardgrounds and phosphorite pebble beds. These phosphorites were dated with strontium isotopes. Major episodes of phosphogenesis occurred between 25 and 16 Ma, and they are coeval with those phosphorite events reported from Florida and North Carolina. A Miocene carbon isotope and oxygen isotope stratigraphy was established on planktic and benthic foraminifera and on bulk samples. A major carbon isotope excursion with an amplitude of up to +1‰ between 18 and 12.5 Ma can be correlated with the globally recognized Monterey carbon isotope excursion. This is the first record of this event both in shallow water sediments and in the Mediterranean. The carbon isotope excursion precedes an oxygen isotope excursion which also was recognized in deep-sea records. Major episodes of phosphogenesis and platform drowning preceded the carbon isotope excursion by up to millions of years.

Introduction

The early-middle Miocene is marked by an excursion in the marine $\delta^{13}C$ record. This C-isotope event is documented in planktic and benthic foraminifera as well as in bulk carbonate carbon isotope records from the Pacific, Atlantic, and Indian Oceans. It is interpreted as an indicator of a major perturbation of the global carbon cycle [*Vincent and Berger*, 1985; *Woodruff and Savin*, 1989; *Hodell*, 1991; *Woodruff and Savin*, 1991; *Hodell and Woodruff*, 1994]. Fluctuations in the global $\delta^{13}C$ record are commonly interpreted as indicators of changing $C_{organic}/C_{carbonate}$ burial rates. *Vincent and Berger* [1985] recognized a link between carbon isotope stratigraphy, organic carbon burial, and phosphogenesis in the Monterey Formation. They explained carbon isotope excursions with changes in upwelling which lead to an increase in organic carbon production and $C_{organic}$ burial. Increased burial of carbon dioxide fixed in organic matter resulted in global cooling. Their Monterey hypothesis has been disputed by *Hodell and Woodruff* [1994] and *Raymo* [1994]. These authors provide a different explanation for the middle Miocene cooling. They postulated that increased silicate weathering related to mountain building resulted in increased CO_2 drawdown. They suggested that increased organic carbon burial may have resulted from elevated nutrient supply by river action.

With this study we contribute to the running debate about the possible links between climate, the phosphorus cycle, and the carbon cycle in the Miocene. The Miocene shelf carbonates outcropping on the Maltese Islands offer the opportunity to reconstruct the response of the Mediterranean to changes in Miocene climate and oceanography. We used planktic and benthic foraminifera and bulk carbonate for the establishment of a central Mediterranean $\delta^{13}C$ and $\delta^{18}O$ record. We also determined Sr-isotopic compositions of carbonates and phosphate peloids in order to date the episodes of phosphogenesis and to correlate them with other phosphate deposits of the world. The Maltese shelf sequences further opened up the unique possibility to relate the $\delta^{13}C$ record with the evolution of a Mediterranean carbonate shelf, with sea level, and with the Miocene carbonate platform drowning.

Geographical and Stratigraphical Setting

The Maltese Islands occupy a central position in the Mediterranean Sea (Figure 1). They are part of the north African continental margin characterized by thick Mesozoic Tertiary carbonates. Exposed are Oligo-Miocene limestones

Paper number 96PA02230.
0883-8305/96/96PA-02230$12.00

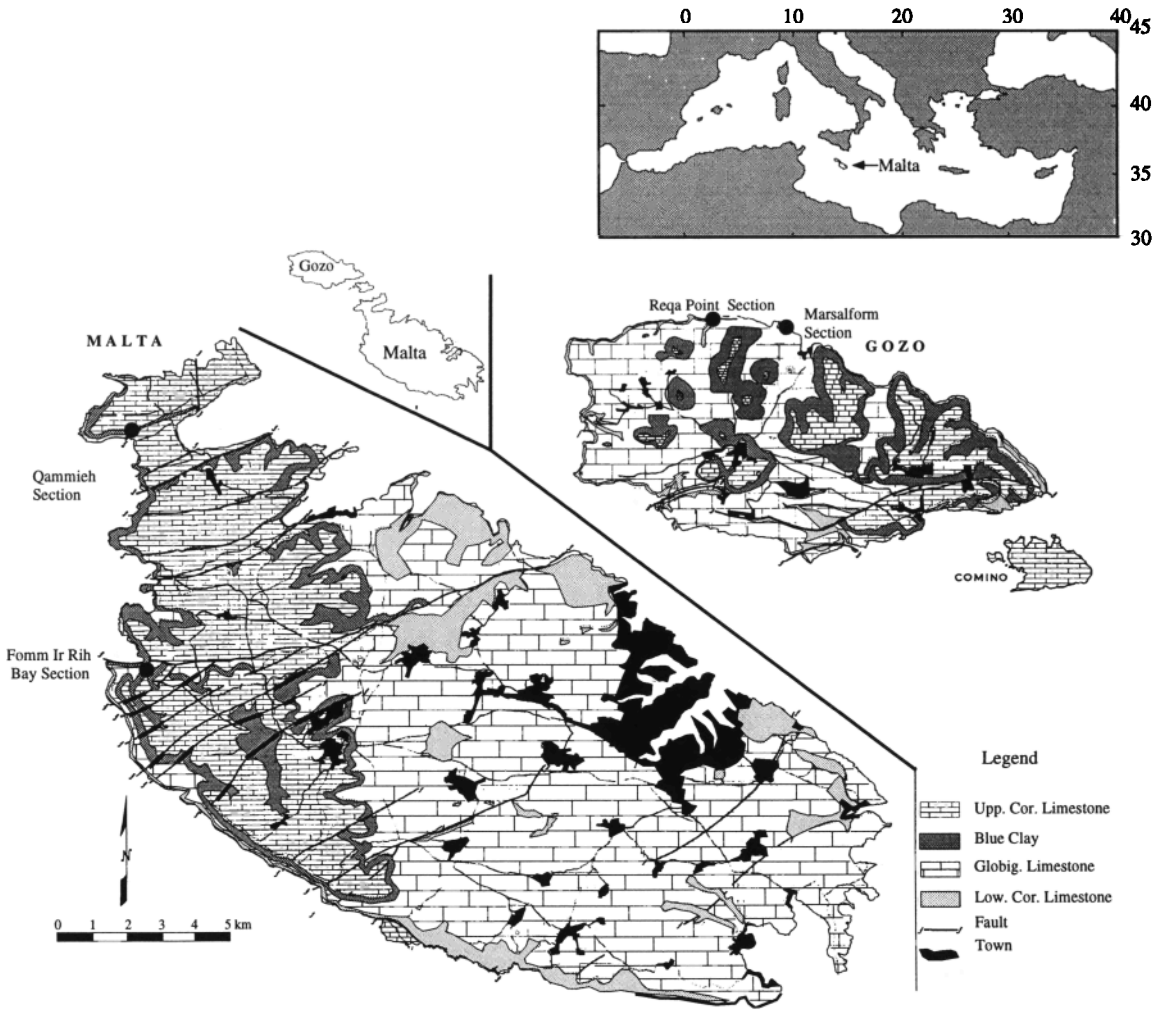

Figure 1. Geographical and geological map of the study area [modified after *Felix,* 1973]. Solid circles indicate locations of the studied sections.

and marls overlain by continental Quaternary deposits. The Tertiary marine sedimentary sequences of Malta and Gozo are divided into five formations: (1) Lower Coralline Limestone Formation, (2) Globigerina Limestone Formation, (3) Blue Clay Formation, (4) Greensand Formation, and (5) Upper Coralline Limestone Formation [*Felix*, 1973]. Despite extensional faulting, these units have more or less retained their original horizontal bedding. The sediments were deposited under relatively shallow water conditions on a shelf extending from Malta to Sicily known as "Ragusa platform" [*Pedley et al.,* 1976]. Water depth in the early Miocene was only a few meters to a few tens of meters, while the sediments of middle Miocene (Langhian-Serravallian) age were deposited at a depth of up to 150-200 m. Very shallow depositional conditions were reestablished in the late Miocene.

Stratigraphy and Sedimentology

The Lower Coralline Limestone forms the base of the sections investigated in Malta and Gozo. It reaches a maximum thickness of about 140 m. The formation is composed mainly of massive limestone beds of shallow marine origin, generally composed of skeletal remains of calcareous algae, benthic foraminifera, corals, bryozoans, brachiopods, serpulids, molluscs, and echinoderms. The formation consists in its lower part of up to 100 m of a yellow, packed biomicrite rich in benthic foraminifera. A pale gray, cross-bedded coralline algal limestone rich in *Lithothamium* and *Archaeolithothamnium* conformably overlies the biomicrites. In eastern Malta, this upper member is replaced by fine-grained biosparites and biomicrites containing a rich foraminiferal fauna of *Lepidocyclina dilatata* and *Heterostegina.* Several horizons with a rich *scutella* fauna mark the top of the formation. The overlying Globigerina limestone consists of a sequence of micritic limestones and marls which may be subdivided into three members: lower, middle, and upper Globigerina limestone [*Felix,* 1973]. These members are separated by two phosphatic nodule beds [*Pedley,* 1975b; *Pedley and Bennett,* 1985]. The lower Globigerina limestone is a yellow to cream, massive bedded, globigerinid biomicrite. Selective cementation of burrows, together with preferential erosion of the surrounding softer sediment, is responsible for the characteristic honeycomb weathering of the unit. The upper

limit of the lower Globigerina limestone is defined by a phosphorite hardground which caps the unit. The fossil content of this phosphorite bed consists of molluscs and clasts, together with sharks teeth. The infauna is restricted to *Chlamys* and the echinoids *Euparagus* and *Spatangus* [*Roman and Roger*, 1939; *Zammit-Maempel*, 1969; *Rose*, 1975].

The middle Globigerina limestone reaches a thickness of about 16 m. It consists of white and pale gray marls and biomicrites. Fossils include echinoids (*S. parkinsoni*, *S. europhytus*) and bivalves (*Chlamys* and *Flabellipecten*). *Thalassinoides* burrow systems are also prominent. At the top of this member, an "upper phosphorite conglomerate bed" is well exposed throughout Malta and Gozo; it consists of about 0.5 m of phosphorite pebbles with additional reworked, phosphatized clasts including the solitary coral *Flabellum*. The upper Globigerina limestone is about 19 m thick; the foraminiferal biomicrites are subdivided into three stratal packages by two phosphorite pebble layers. The macrofauna is sparse and generally restricted to occasional pectinid valves, the echinoid *Schizaster*, and the gastropod *Epitonium* [*Pedley*, 1975a, 1976].

A distinct change from limestone to marl with a low carbonate content of 20 % marks the boundary between the Globigerina Limestone and the Blue Clay Formation. The Blue Clay Formation varies in thickness between some decimeters and up to about 60 m [*Felix*, 1973]. The fossil content of the Blue Clay includes gastropods (*Conus* and *Strombus*); the upper part is particularly rich in planktic and benthic foraminifera. Clay mineralogy of the Globigerina Limestone and Blue Clay Formations was carried out by *Visser* [1991]. The Blue Clay Formation has a higher kaolinite, chlorite, and illite to smectite ratio than the Globigerina Limestone Formation. A level rich in palygorskite marks the boundary between these two formations. The top of the Blue Clay Formation is characterized by an increase in glauconite.

The overlying Greensand Formation is up to 12 m thick, and it consists of a basal clayey part and upper calcareous sequence. The calcareous sequence is composed of a poorly cemented bioclastic and glauconitic limestone. In this facies, large echinoids are present and *Heterostegina* is abundant.

The Upper Coralline Limestone is the youngest Miocene formation. It resembles the Lower Coralline Limestone. The maximum preserved thickness of this unit is about 27 m. A large coralline algal biostrome is well exposed in western Malta and eastern Gozo and occurs at the base of the formation. In other areas the lower part of the Upper Coralline Limestone consists entirely of algal rhodoliths, with thin intercalated layers and lenses of algal debris with echinids and *Pecten*.

The presence of Miliolidae and Peneroplidae observed in the Lower Coralline Limestone Formation indicates a shallow water back reef environment, with water depths not exceeding 30-50 m. The Globigerina Limestone Formation is interpreted as a transgressive facies and, thus represents a deepening of the former carbonate platform. Benthic assemblages in the lower part of the Globigerina Limestone Formation such as *Nonion boueanum* [*Blanc-Vernet*, 1969], which seems to thrive in muddy to finely clastic sediments, indicate water depths between 30 and 70 meters. In the upper part of the Globigerina Limestone Formation the benthic fauna show a trend to a more muddy seawater bottom. This trend continues into the Blue Clay Formation. In the Blue Clay Formation the increase of many benthic foraminifera such as buliminids indicates more open-marine conditions, although buliminid species *Bulimina ovata* and *B. inflata* have been reported from different sequences at water depths of less than 200 m. The abundance of macrofaunal species *Flabellipecten larteti* and *Genota spp.*, also suggests water depths of the order of 150 m. A renewed shallowing in the Maltese sections is marked by the onset of conditions which lead to the deposition of the Greensand Formation. The appearance of *Heterostegina* indicates water depths of less than 70 meters. The renewed shallowing trend continued into the Upper Coralline Limestone Formation. This formation represents a carbonate platform growing in water depths of less than 50 m with calcareous algae and epibenthic foraminifera (*Cibicides lobulatus*). This facies interpretation (Figure 2) agrees with observations made by *Felix* [1973], *Bennett* [1979] and *Pedley and Bennett* [1985].

Methods

Biostratigraphy

The biostratigraphy and chronostratigraphy of the Miocene sequence of the Maltese Islands defined in this study are based mainly on planktic foraminifera and on calcareous nannofossils. On the basis of the zonal scheme of *Blow* [1969] the sediments studied were assigned to the following stages: Aquitanian, Burdigalian, Langhian, Serravallian, and Tortonian (Figure 2). With calcareous nannofossils we identified a Chattian age at the base of the section (lower Globigerina limestone; NP 25). According to the nannofossil biozonation of *Martini* [1971] the Greensand Formation belongs to the biozone (NN6-7; Figure 2).

Sr Isotope Stratigraphy

For Sr-isotope measurements we selected only pure peloidal phosphate grains originating from the major phosphorous horizons on the Maltese Islands. From previous studies we know that these authigenic peloids may be perfectly suited for Sr-isotope stratigraphy [*McArthur et al.*, 1990; *DePaolo and Ingram, 1985; Compton et al.*, 1993; *Stille et al.*, 1994]. Peloids commonly have greater mineralogical uniformity and chemical stability than other phosphate material such as phosphatic brachiopods, fish vertebrae, and bone splinters [*Riggs et al.*, 1996]. After hand-picking the peloids to 99% clean under a binocular microscope, they were washed in 20-100% pure acetic acid. This treatment is intended to remove any Sr-rich calcite overgrowths and did not attack the phosphate itself. After two acid treatments the peloids were individually cleaned in ultrapure water and rubbed free of extraneous material using gloves. One peloid was then chosen for each sample and reacted with <1% HCL "suprapur" in a centrifuge tube for less than 10 min and centrifuged. The leachate was allowed to evaporate overnight, with subsequent concentration of strontium carried out using standard cation-exchange procedures.

Calcitic samples (pecten, brachiopod, and foraminifera shells) were first washed in dilute acetic acid before being dissolved completely in <5% pure acetic acid for no longer than 10 min, before centrifugation and evaporation of the leachate.

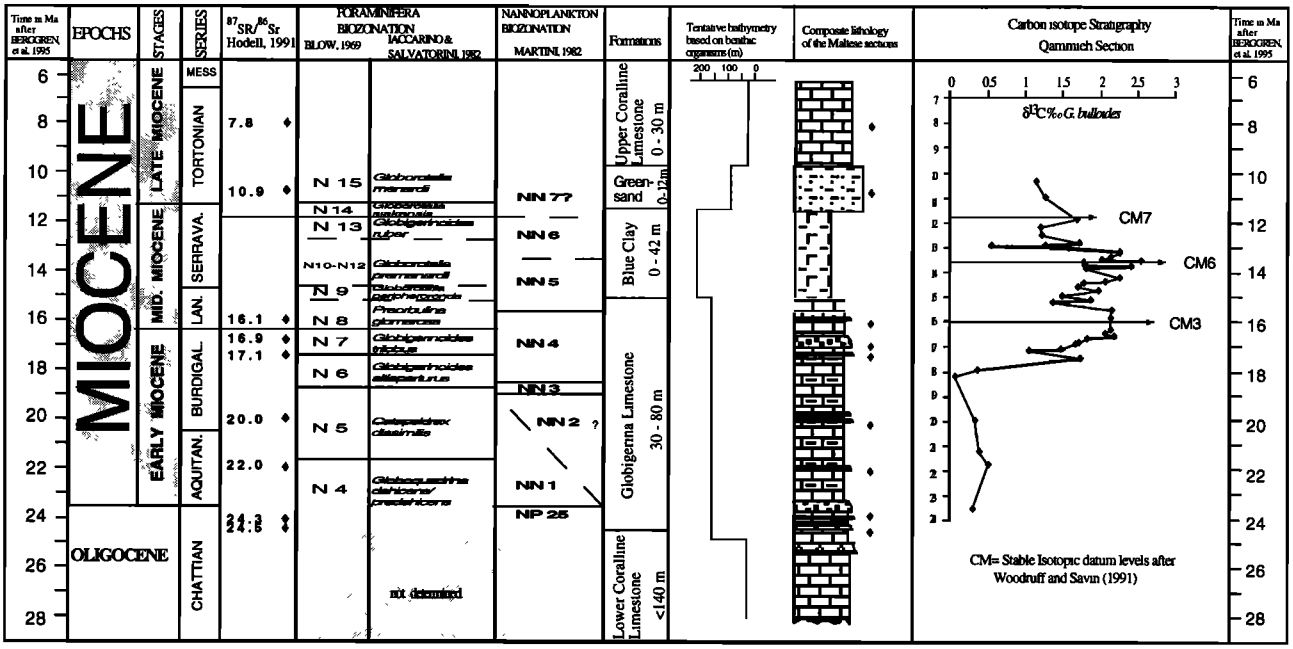

Figure 2. Composite lithostratigraphy and chronostratigraphy of the Maltese sediments based on strontium isotope data, biostratigraphy of planktic foraminifera and calcareous nannofossils and carbon isotope stratigraphy. The bathymetrical interpretation is based on benthic organisms. Strontium isotope samples (denoted by solid diamonds) from 24 to 20 Ma are from the Fomm Ir Rih section (Figure 1) and from 17 to 7 Ma are from the Qammieh section. An additional sample with an age of 16.1 Ma from the Fomm Ir Rih Bay section is plotted (see Figure 1 for location). Strontium ages are cited to the first decimal place only, and errors on these ages can be rounded up to ±0.8 Ma (24 -16.Ma) and ± 1.4 Ma (16-8 Ma), respectively.

Sr-isotope analysis was carried out at the Centre de Géochimie de la Surface (CGS/CNRS) in Strasbourg, France, using the techniques described by *Stille et al.* [1994] and at the Institute of Isotope Geology and Mineral Resources, Eidgenosissche Technische Hochschule Zürich, Switzerland [see *Fischer,* 1988]. At the time the isotope analysis was performed, the NBS 987 standard yielded a $^{87}Sr/^{86}Sr$ value of 0.710269±5 (2σ mean, n=15) at the CGS and 0.710245 ±7 (2σ mean, n=13;) at the ETH.

Carbon and Oxygen Isotope Stratigraphy

Samples for the stable isotope investigation were selected from the Globigerina limestone, from the Blue Clay Formation, and from the Greensand Formation. Sediment samples were desegregated, washed over 315- and 125-μm sieves, and oven dried at 105°C. Pristine specimens of benthic and planktonic foraminifera, common throughout the sequence, were handpicked for carbon and oxygen isotope analysis. Specimens with organic or pyritic fillings or exhibiting phosphatization were discarded. For control purposes, scanning electron microscope photographs were taken and showed no evidence of recrystallization. Approximately 15-20 specimens of planktic and 7-10 specimens of benthic foraminifera representing 250-315 μg of carbonate were required for each measurement. Foraminifera were cleaned in methanol, dried, roasted at 375°C to remove organic contaminants, and reacted in phosphoric acid at 90°C with an on-line-automated carbonate CO_2 preparation device; the evolved CO_2 was cryogenically distilled to remove water produced during the reaction. Samples were run on a VG precision isotope ratio mass spectrometer (PRISM) at the Geologisches Institut ETH, Zürich. Instrumental precision for these analyses of the laboratory standard, Carrara marble (MS-2), was ±0.07‰ for $\delta^{18}O$ and ±0.03‰ for $\delta^{13}C$. Replicate analyses on about one fourth of the samples demonstrated a reproducibility of ±0.04‰ for $\delta^{18}O$ and ±0.02‰ for $\delta^{13}C$. The results[1] are reported relative to the Pee Dee belemnite (PDB) standard (Figures 3-6).

Results

Strontium Isotope Data

The data are compiled in Table 1. In order to compare our data directly with the seawater curve of *Hodell* [1991] we normalized our data to their measured NBS 987 $^{87}Sr/^{86}Sr$ isotopic composition value of 0.710235. The resulting $^{87}Sr/^{86}Sr$ values range between 0.7082 and 0.7089 (Table 1). The corresponding ages were calculated using their isotopic composition values and regression equations for the $^{87}Sr/^{86}Sr$ isotopic composition of seawater as a function of age developed by *Hodell* [1991]. The resolution of strontium isotopic stratigraphy for a given time period is largely dependent upon the rate of $^{87}Sr/^{86}Sr$ increase relative to

[1]Supporting isotope data are available via Anonymous FTP from Kosmos.agu.org, directory APEND (Username = anonymous, Password = guest). Diskette may be ordered from American Geophysical Union, 2000 Florida Avenue, N. W., Washington, DC 20009 or by phone at 800-966-2481; $15.00. Payment must accompany order.

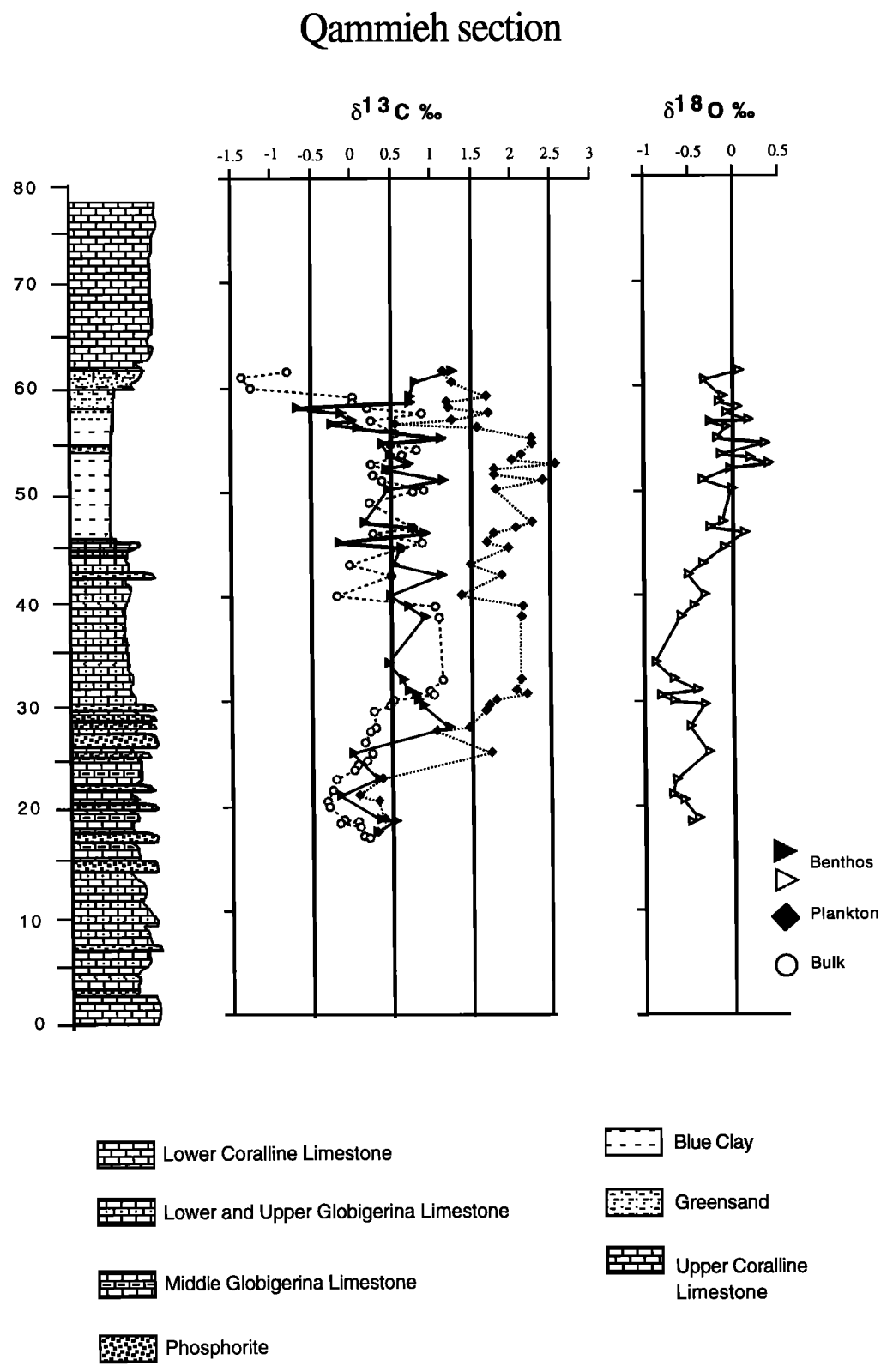

Figure 3. Carbon and oxygen isotopic record of the early and middle Miocene from the Qammieh section, NW Malta. The Monterey carbon isotope excursion is clearly expressed between 20 and 60 m. Open circles denote $\delta^{13}C$ of bulk carbonate, solid squares denote $\delta^{13}C$ of *Globigerinoides bulloides*, and triangles denote $\delta^{13}C$ and $\delta^{18}O$ of *Cibicidoides spp.*

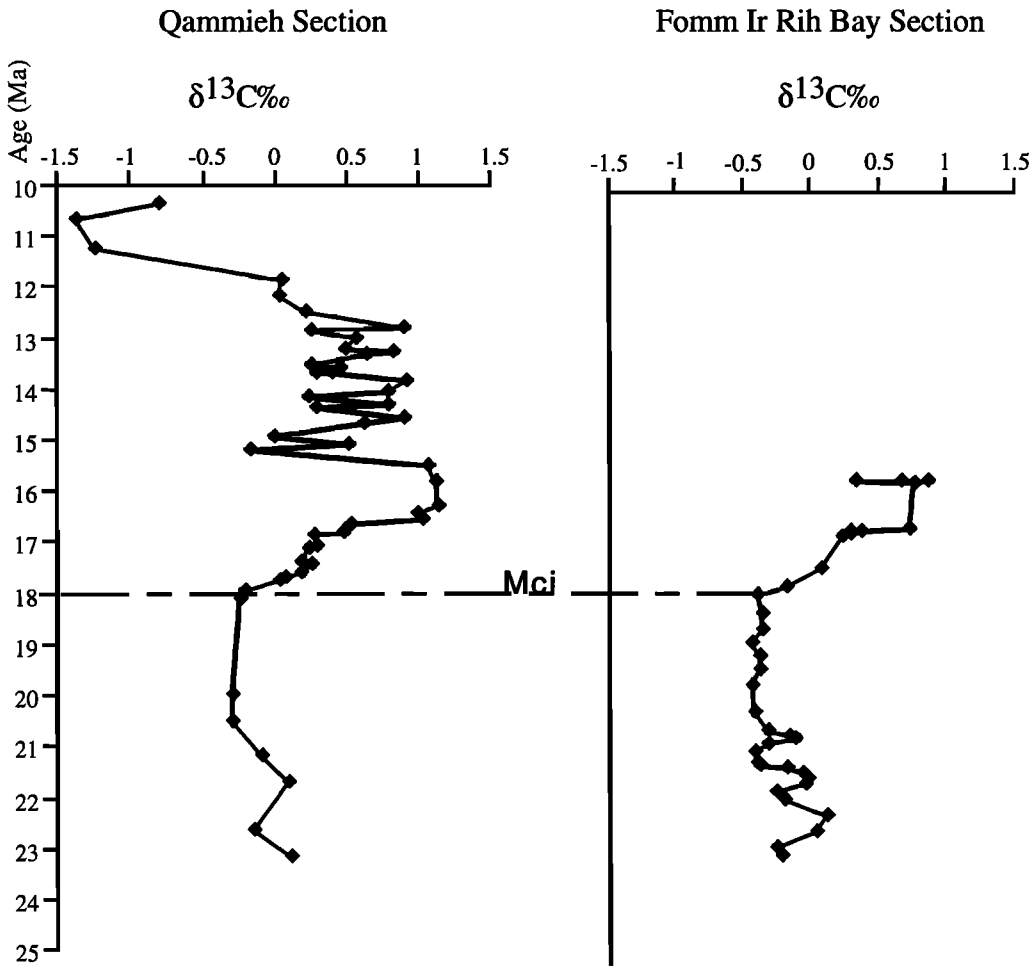

Figure 4. Bulk carbonate carbon isotope record versus age from Qammieh and Fomm Ir Rih Bay sections. The initiation of the Monterey carbon isotope excursion is marked with the dashed line.

analytical error. Using the regression analysis of *Hodell* [1991] the following errors of the Sr age dates have to be considered at the 95% confidence interval: ±0.74 Ma and ±1.36 Ma for the age ranges of 24.0-16 Ma and 16.0-8.0 Ma, respectively. The Sr ages of the phosphate peloids and carbonates are in perfect agreement with the available biostratigraphic ages. This indicates not only that the samples are well preserved but also that the Mediterranean Sea and the oceans were well mixed with respect to Sr-isotopes during this time. Two samples that gave older ages than expected are clearly reworked; they are also from a layer where only very small sparse and different colored peloids were present.

Carbon and Oxygen Isotope Data

The carbon isotopic compositions of the planktic foraminifera *Globigerinoides bulloides* (Figures 3 and 5) fluctuate between +0.2‰ and +0.5‰ during the Aquitanian and early Burdigalian (N4 to N5, lower and middle Globigerina limestone), and increase from + 0.5‰ to + 2‰ in the Burdigalian at 18 Ma. From the middle Burdigalian to the middle Serravallian the $\delta^{13}C$ values scatter around +2‰. Within the Blue Clay Formation at about 12.5 Ma the $\delta^{13}C$ values decrease to +0.5‰. At 13 Ma, during the upper Serravallian, the $\delta^{13}C$ compositions show an increase of almost +1‰, which could represent the beginning of the late Miocene carbon isotope excursion.

In the sediments of Aquitanian age (lower Globigerina limestone) the carbon isotope composition of the benthic foraminifera *Cibicidoides sp.* (Figures 3 and 5) varies between 0‰ and +0.5‰. In the Burdigalian, at 18 Ma the $\delta^{13}C$ values increase from -0.3‰ to +1.3‰. This shift toward more positive values is synchronous with the shift recognized in the planktic foraminifera curve. Relatively positive values persist throughout the Burdigalian, Langhian, and part of the Serravallian. During the Serravallian the $\delta^{13}C$ values decrease again from +1.2‰ to -0.3‰.

At the Burdigalian-Langhian boundary, well preserved foraminifera are rare. This was the reason why the bulk carbonate of the same sections was measured in order to confirm the observed increase of the $\delta^{13}C$ values. In the bulk carbonate curve (Figures 3 and 4) the same +1.5‰ carbon isotope shift was recognized as was in the planktic and benthic foraminifera curve.

The oxygen isotopic composition of the planktic foraminifera *Globigerinoides bulloides* scatters between -0.5‰ and -2‰ in the lower part of the Globigerina limestone (Burdigalian), with no clear trend. From the Burdigalian to the

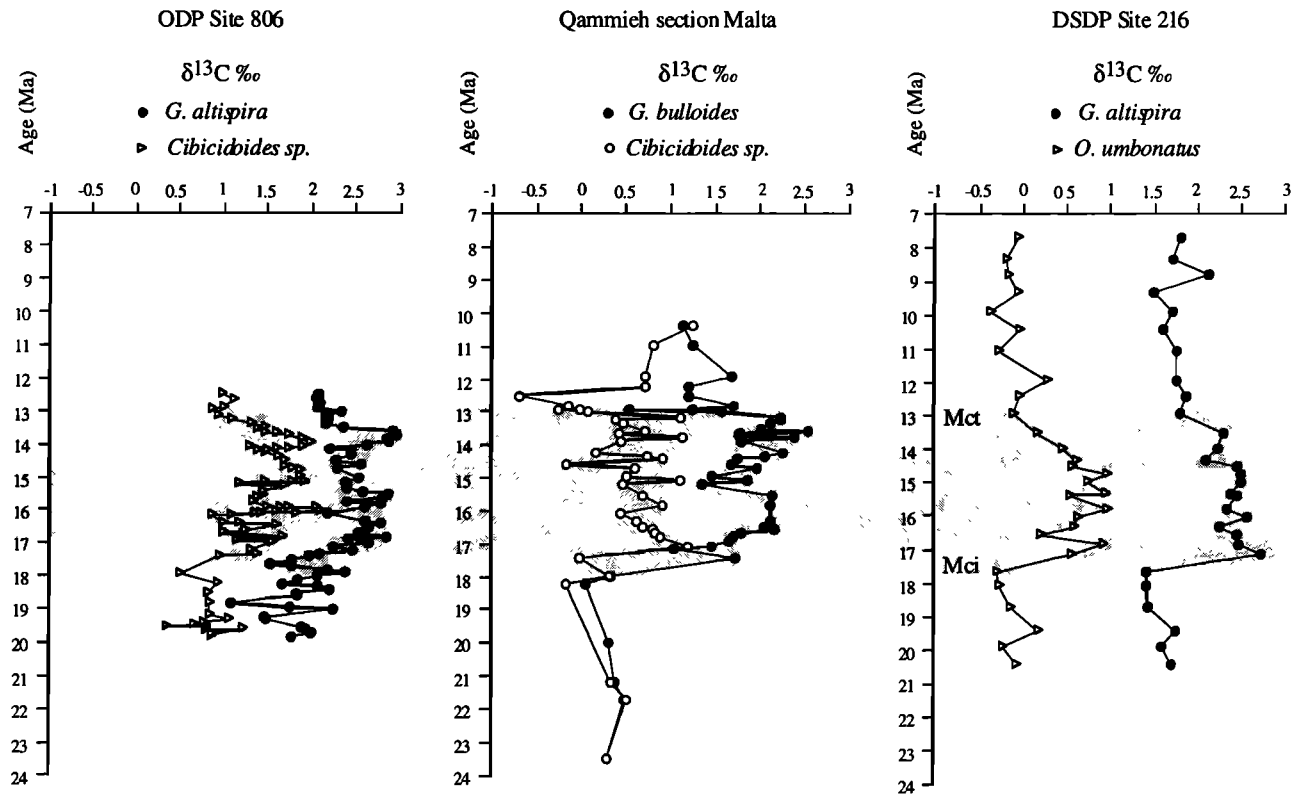

Figure 5. Early and middle Miocene $\delta^{13}C$ record of planktic and benthic foraminifera versus age from southwest Pacific (ODP Site 806 [*Corfield and Cartlidge,* 1993]; solid circles denote $\delta^{13}C$ of *G. altispira* and open triangles denote $\delta^{13}C$ of *Cibicidoides sp.*); Malta (solid circles denote $\delta^{13}C$ of *G. bulloides* and open circles denote $\delta^{13}C$ of *Cibicoides sp.*); and the tropical Indian Ocean (DSDP Site 216 [*Vincent and Berger,* 1985]; solid circles denote $\delta^{13}C$ of *G. altispira* and open triangles denote $\delta^{13}C$ of *O. umbonatus*). Results are reported relative to the PDB standard. The shaded interval represents the initiation (Mci) and termination (Mct) of the Monterey carbon isotope excursion.

lower part of the Serravallian the $\delta^{18}O$ values scatter around -1.5‰. In the lower part of the Serravallian the oxygen isotopic composition decreases to -2.5‰. Then the composition increases from -2.5‰ to -1‰ during the middle and upper Serravallian. At 13 Ma the $\delta^{18}O$ values show a decrease from -1‰ to -2.5‰ before they increase again from -2.5‰ to -0.5‰ in the lower part of the Tortonian.

Between 22 and 17 Ma the oxygen isotopic composition of the benthic foraminifera *Cibicidoides sp.* (Figure 6) scatters between -0.6‰ and -0.3‰. At 17 Ma the $\delta^{18}O$ values decrease to -0.8‰. Starting at 16 Ma, the $\delta^{18}O$ values increase gradually from -0.8‰ to +0.3‰ within the lower part of the Blue Clay Formation. This shift represents the initiation of the middle Miocene cooling step associated with the Antarctic ice build up [*Woodruff and Savin,* 1989].

The bulk carbonate of the Qammieh section shows a pronounced shift in the $\delta^{18}O$ values from -1.8‰ to +0.5‰ at about 23 Ma and then a sharp decrease to -1.5‰ in the lower part of the Globigerina limestone. At 18 Ma the $\delta^{18}O$ values increase gradually from -1.3‰ to +0.2‰ within the Blue Clay Formation and decrease again from +0.2‰ to -1‰ at 13 Ma.

Discussion

Our investigations of the Oligo-Miocene carbonate platform and shelf sediments on Malta allow us to draw a picture of the Miocene paleoceanography of the central Mediterranean. We are able to link it with changes in global carbon cycling and climate as recorded in carbon and oxygen isotope stratigraphies. Biostratigraphy, combined with Sr-isotope stratigraphy, provides an accurate time frame which facilitates the correlation of the Mediterranean record with platform and shelf sequences in other oceans and with Miocene deep-sea records.

The Malta sequence records a change from carbonate platform conditions to shelf environments in the Late Oligocene. The micritic foraminifera limestone facies of the Globigerina limestone was deposited on a deepening and episodically current swept shelf. Hardgrounds were formed during these episodes. Phosphorite crusts and pebbly phosphorite beds represent periods of no net sediment accumulation [*Pedley and Bennett,* 1985]. The present-day Peru margin [*Burnett,* 1977] with its phosphorite hardgrounds may

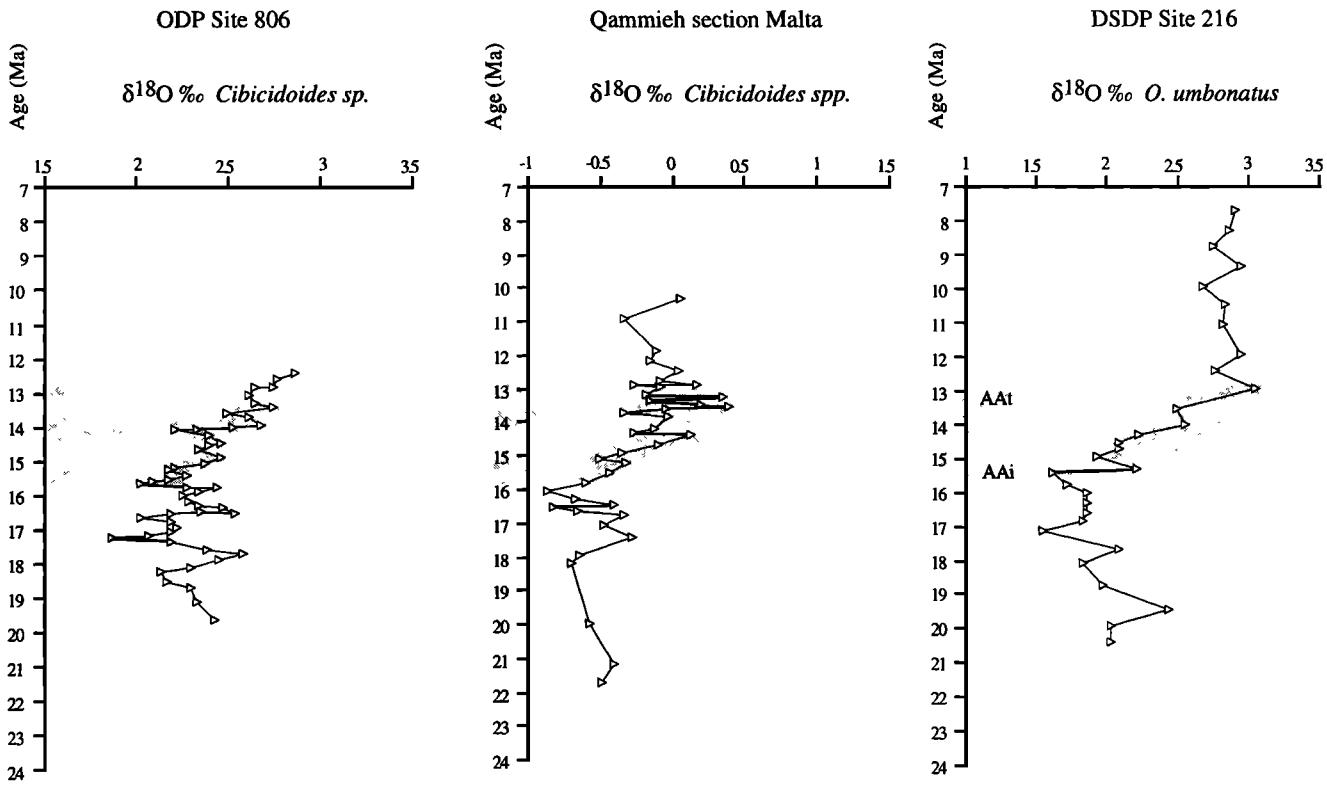

Figure 6. Early and middle Miocene $\delta^{18}O$ record of benthic foraminifera versus age from southwest Pacific (ODP Site 806 [*Corfield and Cartlidge,* 1993], Malta, and the tropical Indian Ocean (DSDP Site 216 [*Vincent and Berger,* 1985]. Results are reported relative to the PDB standard. The shaded interval represents the initiation (AAi) and termination (AAt) of the Antarctic cooling episode.

serve as an actualistic example for the Miocene phosphorites which formed on the Malta-Ragusa shelf. The first major phosphorite bed, separating the lower from the middle Globigerina limestone, marks a distinct change in the benthic fauna, indicating a deepening of the Malta shelf. On the basis of these observations we conclude that the major phosphorite layers were formed at times of relative sea level rise and that platform drowning and successive deepening of the shelf occurred stepwise. The deepening upward trend recognized in the Globigerina Limestone Formation reached its maximum during the deposition of the Blue Clay Formation, which may have been deposited in a depth of up to 200 m. The deepening of the shelf was accompanied by a change in carbonate content of the shelf sediments. Low carbonate contents of about 20% in the Blue Clay Formation seem to reflect a combination of increased dilution of the carbonate by detrital clay, decreased carbonate production, and increased dissolution of carbonate. The clay mineralogy of the Blue Clay Formation indicates a trend to more humid climate, resulting in intensified weathering, runoff, and transfer of fine siliciclastics into the central Mediterranean. If we combine the sedimentological information of the upper part of the Globigerina Limestone and Blue Clay Formations with the benthic C-isotope signatures, we may conclude that an expanded oxygen minimum layer extended across the Malta shelf between 16 and 12 Ma. The shallow position of the oxygen minimum zone along the Peru margin could serve as an actualistic analog of the Malta situation [*Burnett,* 1977]. The deepening upward trend of the Malta shelf was reversed in the late Miocene. The Greensand and Upper Coralline Limestone Formations record a renewed shallowing upward of the Malta shelf and the reestablishment of carbonate platform conditions 12 Ma after the inital drowning phase.

The sedimentological evolution of the Malta shelf shows remarkable analogies to the record of the western North Atlantic (Figure 7). The major episodes of phosphogenesis on the Malta shelf occurred between 24 and 16 Ma and can be correlated with synchronous episodes of phosphogenesis along the western North Atlantic [*Compton et al.,* 1990 and 1993; *Stille et al.,* 1994]. In agreement with *Compton et al.,* [1990], we consider a rise in sea level as one factor favoring the formation of phosphorite beds. Comparisons with Cretaceous records indicate that conditions for phosphogenesis were most favorable when specific paleoceanographic conditions coincided with times of accelerated weathering, erosion and transfer of nutrients from continents into oceans [e.g., *Weissert,* 1989; *Föllmi et al.,* 1994; *Raymo,* 1994].

Increased nutrient loads had an impact not only on the marine phosphorus budget but also on the marine carbon system. The Miocene C-isotope record shows how the rain rate of organic carbon to carbonate carbon was altered on a global scale beween 18 and 12 Ma. The C-isotope excursion, as we identified it in the Malta archives, started at 18 Ma. It reached its most positive values around 17 Ma, and it ended about 12.5

Table 1. $^{87}Sr/^{86}Sr$ Measurements and Derived Ages of Samples From Malta

Sample	$^{87}Sr/^{86}Sr$ Mean Values[a]	$^{87}Sr/^{86}Sr$ of *Hodell* [1991][b]	Age,[c] Ma
	Qammieh Section		
Qab 2[d] (LCL)[e]	0.708254 (14)	0.708244	24.00
Qab 3 (GL)	0.708245 (6)	0.708211	24.54
Qab 4 (GL)	0.708276 (7)	0.708242	24.03
Qab 28 (GL)	0.708692 (6)	0.708658	17.16
Qab 29 (GL)	0.708682 (7)	0.708648	17.32[f]
Qab 30 (GL)	0.708700 (6)	0.708666	17.03
Qab 31 (GL)	0.708704 (7)	0.708669	16.96
Qab 39 (GL)	0.708253 (7)	0.708219	24.41[f]
Qabb 19[g] (BC)	0.70885 (18)	0.70884	10.87
LCL[d] (LCL)	0.708256 (6)	0.708222	24.36
UCL[i] (UCL)	0.708946 (6)	0.708912	7.81
	Fomm Ir Rih Bay Section		
FG 5 (GL)	0.708246 (6)	0.708212	24.53
FG 7 (GL)	0.708254 (7)	0.708220	24.39
FG 8 (GL)	0.708260 (6)	0.708226	24.30
FG 17 (GL)	0.708400 (6)	0.708366	21.98
FG 20[d] (GL)	0.708496 (11)	0.708486	20.00
FG 41 (GL)	0.708697 (8)	0.708663	17.08
FG43 (GL)	0.708754 (6)	0.708720	16.14
	Reqa Point and Marsalform Sections		
RP 14 (LCL)	0.708290 (7)	0.708256	23.80
MAR_{bottom} (GL)	0.708676 (6)	0.708642	17.42
MAR_{top} (GL)	0.708689 (7)	0.708655	17.20
MAR 0 (GL)	0.708277 (7)	0.708243	24.02
	Il Gelmus Section		
IG8 (GR)	0.709036 (7)	0.709002	6.3

Formation abbreviations are LCL, Lower Coralline Limestone; GL, Globigerina Limestone; BC, Blue Clay; GR, Greensand; UCL, Upper Coralline Limestone.
Uncertainties in brackets of the Sr isotopic compositions are at the 2σ mean level.
[a]NBS 987:0.710269 (Str) 0.710245 (ETH).
[b]NBS 987:0.710235.
[c]After correction to *Hodell's* [1991] NBS 987.
[d]Pectinids.
[e]Samples were measured at ETH, Zürich.
[f]Interpreted to be reworked phosphate peloids being particurlarly small and from levels where there are only sparse peloids.
[g]Foraminifera.
[h]Two foram fractions were measured.
[i]Brachiopod.

Ma. The synchroneity of the Malta C-isotope excursion with pelagic C-isotope records confirms the global extent of the Miocene Monterey event in C-isotope stratigraphy.

While the amplitude of planktic record is comparable with records from the Pacific and Indian Oceans, the benthic C-isotope excursion is marked by a low amplitude change. We interpet this discrepancy with the peculiar environment of deposition of the Blue Clay Formation. At the time of globally most positive C-isotope values, benthic foraminifera on the Malta shelf lived within an expanded oxygen minimum layer. An expanded oxygen minimum layer enriched with isotopically light CO_2 would have resulted in a negative shift of the benthic C-isotope signal. This negative shift may have partly compensated the globally recognized positive shift of mid-Miocene ocean water.

The C-isotope excursion is commonly interpreted as an indicator of increased burial of organic carbon. Increased nutrient loads not only may have resulted in an intensification of the marine organic carbon pump, but they may also have had an impact on the marine carbonate carbon burial rate. Coastal regions and shelves affected by elevated nutrient loads may have experienced growth crises resulting in platform

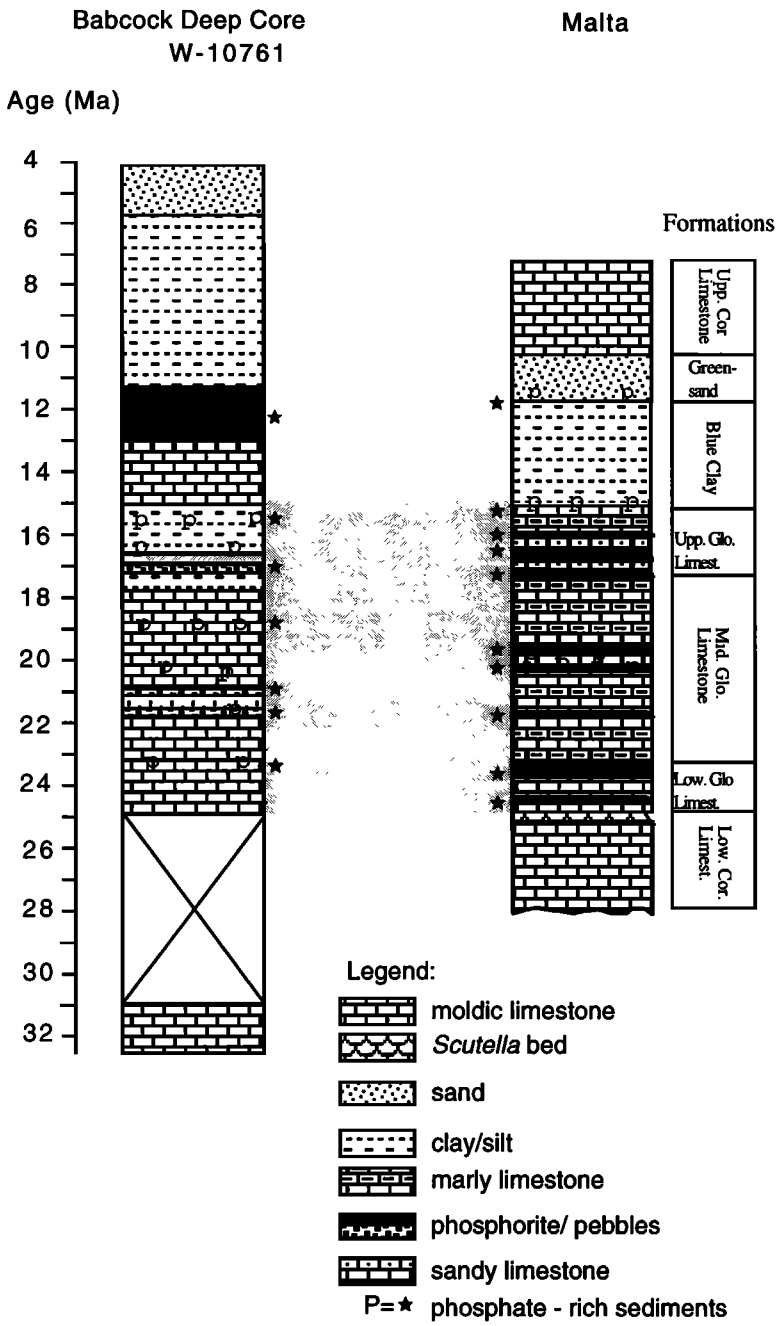

Figure 7. Comparison of major episodes of phosphogenesis with lithostratigraphy. Data are from the Babcock Deep Core South-Central Florida Platform [*Compton et al.*, 1993]. The shaded interval represents major episodes of phosphogenesis between 25 and 15 Ma.

drowning and in regionally decreased carbonate sedimentation. This may explain why the increase in global organic carbon burial rates was not fully compensated by an equally large increase in carbonate carbon burial rate as reflected in the altered $C_{organic}/C_{carbonate}$ burial ratio. If we accept that growth crises of carbonate platforms during times of rising sea level may influence the carbonate carbon pump, then the C-isotope excursion in the Miocene reflects a major perturbation of both marine carbon pumps. In this context it seems remarkable that the end of the Miocene C-isotope excursion coincides with a shallowing upward trend of the Malta-Ragusa shelf. This reflects an improved growth potential of Mediterranean carbonate platforms in the late Miocene, and it could have contributed to the renewed decrease in $C_{organic}/C_{carbonate}$ burial rate as reflected in decreasing $\delta^{13}C$ values. An analogous link between carbonate carbon burial rates and the C-isotope record has recently been suggested by *Weissert and Mohr* [1996] for the Late Jurassic and Early Cretaceous time intervals.

Variations in carbon burial rates had an impact on the atmospheric CO_2 reservoirs, as discussed by *Vincent and Berger* [1985] for the Monterey event. The Malta sediments

provide us with an oxygen istope curve which can be compared with the deep-sea records. The early Miocene (20-17 Ma) oxygen isotope curve shows minor fluctuations. This agrees with records from the Pacific and Atlantic Oceans (Figure 6). From 17 to 15.5 Ma the oxygen isotopic composition of Malta shows a decrease of 0.5‰, indicating a phase of global warming. This decrease correlates with the one reported in Site 747 ranging from 17 to 15.5 Ma. *Hodell and Woodruff* [1994] attributed this decrease to the major eruption phase of the Columbia River Flood Basalt. After 15.5 Ma the $\delta^{18}O$ curve shifts toward more positive values. The most positive $\delta^{18}O$ values at 15 Ma correlate with the maximum peak observed in the $\delta^{13}C$ record. These $\delta^{18}O$ values are interpreted to be the result of a middle Miocene cooling step associated with the Antarctic ice buildup [*Woodruff and Savin,* 1989]. If we compare the carbon isotope curve with the oxygen isotope record, we recognize a considerable time lag of up to 2 Ma between the initiation of the carbon isotope excursion and the shift in the oxygen isotope record to more positive values. This observation is in agreement with data from the Indian and Pacific Oceans [*Vincent and Berger*, 1985; *Corfield and Cartlidge,* 1993] and it may reflect a reduction in atmospheric CO_2 levels due to increased global weathering and/or to an intensification of the marine carbon pumps [*Hodell and Woodruff,* 1994; *Vincent and Berger,* 1985; *Raymo,* 1994].

From 13 to 11 Ma the $\delta^{18}O$ values of Malta (Figure 6) show a gradual decrease by about 1‰, which is not observed in deep-sea sequences. This may be the local expression of the isolation of the Mediterranean Sea from the Indo-Pacifc Ocean. Today the Mediterranean Sea is a basin with an anti-estuarine circulation (surface inflow with outflow at depth). The oxygen isotope record of different deep-sea sequences from the Atlantic, Indian, Pacific, and Southern Oceans show that deep water temperatures at 12.5 Ma can be explained by deep water circulation changes. *Wright and Miller* [1992] argued that the Northern Component Water and Southern Component Intermediate Water were produced from 12.5 to 10 Ma and reflect an oceanic circulation pattern similar to today. Assuming that at 12.5 Ma the Mediterranean Sea was closed from the Indian Ocean, an increasing influx of fresh water and changes in temperature and/or salinity may have produced a decrease in the oxygen isotopic composition of deep water as it is observed in the Maltese sections.

Conclusions

Miocene shallow water sediments outcropping on the Maltese Islands provide an excellent archive of Miocene paleoceanography. On the basis of sedimentological and paleontological evidence, we may conclude that the Miocene Malta-Ragusa platform experienced a stepwide deepening between 25 and 15 Ma. Phosphorite hardgrounds formed on the deepening shelf mark episodes of sea level rise. The Blue Clay Formation deposited between 15.5 and 12 Ma and at a water depth near 200 m reflects the deepest conditions of the Malta shelf before a carbonate platform was reestablished at about 12 Ma. Using Sr-isotope stratigraphy, we are able to date major episodes of phosphogenesis between 24 and 17 Ma. These were coeval with analogous episodes of phosphogenesis on the Florida and North Carolina shelves. We have established a Miocene C-isotope curve on planktic and benthic foraminifera and on bulk samples, and we can document how the major Montery C-isotope event followed the episodes of phosphogenesis with a lag of up to millions of years. The maximum of the C-isotope excursion at 16 Ma coincided with the deposition of the upper Globigerina limestone and Blue Clay Formation and with the onset of global mid-Miocene cooling as indicated in the O-isotope record. The Mediterranean O-isotope curve not only records changes in global climate, but a shift to isotopically lighter values also reflects the closure of the Mediterranean from the Indo-Pacific Ocean between 13 and 11 Ma.

Acknowledgments. The authors thank M. Pika-Biolzi and K. Perch-Nielsen (ETH Zürich) for biostratigraphic advice. I. Stössel, S. Bernasconi, and D. Bernoulli (ETH Zürich) provided very helpful criticism and comments, which are gratefully acknowledged. We acknowledge the continuous support of H. R. Thierstein (ETH Zürich) and B. Mohr (Museum für Naturkunde Berlin). Many thanks to B. Kiefel and D. Tisserand at the CGS/CNRS in Strasbourg for their invaluable help in the laboratory. We have especially appreciated the continued interest and help of G. Zammit-Maempel on all matters relating to the geology of the islands. Constructive reviews by J. Compton, B. Garrison and L. Derry helped to improve the manuscript. This research was supported by the Swiss National Science Foundation grant NSF 20-36555.92.

References

Bennett, S.M., A transgressive carbonate sequence spanning the Paleogene-Neogene boundary on the Maltese Islands, *Ann. Geol. Pays Hell.*, Tome horse ser. *1*, 71-80, 1979.

Blanc-Vernet, L., Contribution à l'étude des foraminifères de la Méditerraée: Relations entre le microfaune et le sédiment: Biocoenoses actuelles, thanatocoenoses pliocènes et quaternaires, *Rec. Trav. Strat. Mar. d'Etoume, 64*, 281, 1969.

Blow, W.H., Late Middle Eocene to recent plankonic foraminiferal biostratigraphy, *Proc. Int. Conf. Plank. Microfossils, 1*, 199-442, 1969.

Burnett, W.C., Geochemistry and origin of phosphorite deposits from Peru and Chile, *Bull. Geol. Soc. Am., 88*, 813-823, 1977.

Compton, J., S.W., Snyder, and D., Hodell, Phosphogenesis and weathering shelf sediments from SE USA: Implications for Miocene $\delta^{13}C$ excursion and global cooling, *Geology, 18*, 1227-1230, 1990.

Compton, J.S., D.A., Hodell, J.R., Garrido, and D.J., Mallinson, Origin and age of phosphorite from the south-central Florida Platform: Relation of phosphogenesis to sea-level fluctuations and $\delta^{13}C$ excursions, *Geochim. Cosmchim. Acta., 57*, 131-146, 1993.

Corfield, R.M., and J.E., Cartlidge, Oxygen and carbon isotope stratigraphy of the middle Miocene, Holes 805B and 806B, *in Proc. Ocean Drill. Program, Sci. Res., 130*, 307-322, 1993

DePaolo, D.J., and B.L., Ingram, High-resolution stratigraphy with strontium isotopes, *Science, 227*, 938-941, 1985.

Felix, R., Oligo-Miocene stratigraphy of Malta and Gozo, Ph.D. dissertation, Univ. of Utrecht, Utrecht, Netherlands, 1973.

Fischer, H., Isotopengeochemische Untersuchungen und Datierungen an Mineralien und Fossilien aus Sedimentgesteinen, Ph.D. dissertation, Eidgenossische Technische Hochschule Zürich, Switzerland, 1988.

Föllmi, K.B., H., Weissert, M., Bisping, and H., Funk, Phosphogenesis, carbon-isotope stratigraphy, and carbonate-platform evolution along the Lower Cretaceous northern Tethyan margin, *Bull., Geol. Soc. Am., 106*, 729-746, 1994.

Hodell, D. A., Variations in the strontium isotopic composition of seawater during the Neogene, *Geology, 19*, 24-27, 1991.

Hodell, D.A., and F., Woodruff, Variations in the strontium isotopic ratio of seawater during the Miocene: Stratigraphic

and geochemical implications, *Paleoceanography*, *9*, 405-426, 1994.

Martini, E., Standard Tertiary and Quaternary calcareous nannoplankton zonation, *Proc. Plank. Conf. Roma*, *2*, 739-785, 1971.

McArthur, J.M., A.R., Sahami, M.F., Thirwall, A.O., Osborn, and P.J., Hamilton, Dating phosphogenesis with Sr-isotopes: *Geochim. Cosmochim. Acta*, *54*, 1343-1351, 1990.

Pedley, H.M., Miocene sea-floor subsidence and Later subaerial solution subsidence structures in the Maltese Islands, *Proc. Geol. Ass.*, *85*, 533-547,.1975a.

Pedley, H.M., The Oligo-Miocene sediments of the Maltese Islands, Ph.D., dissertation, Univ. of Hull, Hull, England, 1975b.

Pedley, H.M., and S.M., Bennett, Phosphorites, hardgrounds and syndepositional solution subsidence: A paleoenvironmental model from the Miocene of the Maltese Islands, *Sediment. Geol.*, *45*, 1-34, 1985.

Pedley, H.M., M.R., House, and B., Waugh, The Geology of Malta and Gozo, *Proc. Geol. Assoc.*, *87*, 321-341, 1976.

Raymo, M.E., The Himalayas, organic carbon burial, and climate in the Miocene, *Paleoceanography*, *9*, 399-404, 1994.

Riggs, S., P., Stille, and D., Ames, Sr isotopic age analysis of co-occuring Miocene phosphate grain types on the North Carolina continental shelf, *J. Sediment. Petrol.*, in press, 1996.

Roman, F., and J., Roger, Observations sur la faune de Pectinides de Malte, *Bull. Soc. Géol. Fr.*, *5*, 59-67, 1939.

Rose, E.P.F., Oligo-Miocene echinoids of the Maltese Islands, *Proc. VIth Cong. Reg. Comit. Med. Neog. Stra.*, *1*, 75-79, 1975.

Stille, P., S., Riggs, N., Clauer, D., Ames, R., Crowson, and S., Snyder, Sr and Nd isotopic analysis of phosphorite sedimentation through one Miocene high-frequency depositional cycle on the North Carolina continental shelf, *Mar. Geol.*, *117*, 253-23, 1994.

Vincent, E., and W. H., Berger, Carbon dioxide and polar cooling in the Miocene; The Monterey Hypothesis, in *The Carbon Cycle and Atmospheric CO_2: Natural Variations Archean to Present*, *Geophys. Monogr.*, Ser. vol. 32, edited by E.T. Sundquist and W. S. Broecker, pp.455-468, AGU, Washington, D. C., 1985.

Visser, J.P., Clay mineral stratigraphy of Miocene to Recent marine sediments in the central Mediterranean, *Geol. Ultraiectina*, *75*, 243, 1991.

Weissert, H., C-Isotope stratigraphy, a monitor of paleoenvironmental change: A case study from the Early Cretaceous: *Surv. Geophys.*, *10*, 1-61, 1989.

Weissert, H.J., and H., Mohr, Late Jurassic Climate and its impact on carbon cycling, *Palaeogeogr. Palaeoclimatol. Palaeoecol.*, *122*, 27-43, 1996.

Woodruff, F., and S. M., Savin, Miocene deepwater oceanography, *Paleoceanography*, *4*, 87-140, 1989.

Woodruff, F., and S.M., Savin, Mid-Miocene isotope stratigraphy in the deep sea: High-resolution correlations, paleoclimatic cycles, and sediment preservation, *Paleoceanography*, *6*, 755-806, 1991.

Wright, J.D., and K.G., Miller, Miocene stable isotope stratigraphy, site 747, Kerguelen Plateau: *Proc. Ocean Drill Program, Sci. Results*, *120*, 855-866, 1992.

Zammit-Maempel, G., A new species of Coeloplerus (Echinoidea) from the Miocene of Malta, *Paleontology*, *12*, 42-47, 1969.

E. Jacobs, G. Shields, and H. Weissert, Geological Institute, Swiss Federal Institute of Technology, CH-8092 Zürich, Switzerland.

P. Stille, CNRS, Centre de Geochemie de la Surface, F-60784, Strasbourg, France.

(Received December 29, 1995; revised July 19, 1996; accepted July 19, 1996.)